Cellular and Molecular Life Sciences (2022) 79:246
https://doi.org/10.1007/s00018-022-04267-5

ORIGINAL ARTICLE

Molecular mechanisms of aberrant neutrophil differentiation in glycogen storage disease type Ib

Sang Wan Sim[1] · Yuyeon Jang[1] · Tae Sub Park[2] · Byung-Chul Park[2] · Young Mok Lee[3] · Hyun Sik Jun[1]

Received: 18 January 2022 / Revised: 4 March 2022 / Accepted: 21 March 2022 / Published online: 18 April 2022

Abstract

Glycogen storage disease type Ib (GSD-Ib), characterized by impaired glucose homeostasis, neutropenia, and neutrophil dysfunction, is caused by a deficiency in glucose-6-phosphate transporter (G6PT). Neutropenia in GSD-Ib has been known to result from enhanced apoptosis of neutrophils. However, it has also been raised that neutrophil maturation arrest in the bone marrow would contribute to neutropenia. We now show that *G6pt*$^{-/-}$ mice exhibit severe neutropenia and impaired neutrophil differentiation in the bone marrow. To investigate the role of G6PT in myeloid progenitor cells, the *G6PT* gene was mutated using CRISPR/Cas9 system, and single cell-derived *G6PT*$^{-/-}$ human promyelocyte HL-60 cell lines were established. The *G6PT*$^{-/-}$ HL-60s exhibited impaired neutrophil differentiation, which is associated with two mechanisms: (i) abnormal lipid metabolism causing a delayed metabolic reprogramming and (ii) reduced nuclear transcriptional activity of peroxisome proliferator-activated receptor-γ (PPARγ) in *G6PT*$^{-/-}$ HL-60s. In this study, we demonstrated that G6PT is essential for neutrophil differentiation of myeloid progenitor cells and regulates PPARγ activity.

Keywords Myeloid progenitor cells · Glucose-6-phosphate transporter · CRISPR/Cas9 · Peroxisome proliferator-activated receptor-γ

Abbreviations

1,5-AG6P	1,5-Anhydroglucitol-6-phosphate
AAV8	Adeno-associated virus serotype 8
BM	Bone marrow
CEBP	CCAT/enhancer-binding protein
ECAR	Extracellular acidification rate
ER	Endoplasmic reticulum
ERK1/2	Extracellular signal-regulated kinase 1/2
FAO	Fatty acid oxidation
G-CSF	Granulocyte-colony-stimulating factor
G-CSFR	Granulocyte-colony-stimulating factor receptor
G6P	Glucose-6-phosphate
G6Pase	Glucose-6-phosphatase
G6PT	Glucose-6-phosphate transporter
GFI1	Growth factor independent 1 transcriptional repressor
GSD-Ib	Glycogen storage disease type Ib
HIF-1α	Hypoxia-inducible factor-1-α
OCR	Oxygen consumption rate
OXPHOS	Oxidative phosphorylation
PARP	Poly (ADP-ribose) polymerase
PPARα	Peroxisome proliferator-activated receptor-α
PPARγ	Peroxisome proliferator-activated receptor-γ
SIRT1	NAD-dependent protein deacetylase sirtuin 1

Introduction

Glycogen storage disease type Ib (GSD-Ib) is an autosomal-recessive syndrome characterized by impaired glucose homeostasis, neutropenia, and neutrophil dysfunction [1, 2].

Hyun Sik Jun is a lead author between the two corresponding authors.

✉ Young Mok Lee
yolee@uchc.edu

✉ Hyun Sik Jun
toddjun@korea.ac.kr

[1] Department of Biotechnology and Bioinformatics, College of Science and Technology, Korea University, Sejong 339-700, Republic of Korea

[2] Graduate School of International Agricultural Technology, and Institute of Green-Bio Science and Technology, Seoul National University, Pyeongchang, Gangwon 25354, Republic of Korea

[3] Department of Pediatrics, University of Connecticut School of Medicine, Farmington, CT 06030, USA

GSD-Ib is caused by a mutation in the *SLC37A4* gene that results in disruption of the activity of glucose-6-phosphate (G6P) transporter (G6PT) [3]. G6PT transports G6P from the cytoplasm into the lumen of the endoplasmic reticulum (ER), where it is hydrolyzed into glucose and phosphate by glucose-6-phosphatase-α (G6Pase-α) or glucose-6-phosphatase-β (G6Pase-β) [1, 4]. GSD-Ib is characterized by hypoglycemia, accumulation of excessive glycogen, growth retardation, hyperlipidemia, neutropenia, and myeloid dysfunctions [5, 6]. It has been shown that G6PT deficiency causes ER and mitochondrial oxidative stress-induced apoptosis that leads to neutropenia and impaired energy homeostasis, which underlies neutrophil dysfunction such as impaired respiratory burst, chemotaxis, and calcium mobilization activities [7]. In addition to apoptosis of neutrophils, several studies have shown that neutrophil maturation arrest in the bone marrow (BM) of some GSD-Ib patients might also contribute to neutropenia [8].

Granulocyte-colony stimulating factor (G-CSF) is widely used to increase absolute neutrophil counts and prevent bacterial infections in GSD-Ib patients. However, it has been reported that G-CSF therapy does not rescue the impairment in neutrophil migration and adhesion in *G6pt*$^{-/-}$ mice [9]. Furthermore, long-term treatment with G-CSF might lead to acute myeloid leukemia or myelodysplastic syndromes, suggesting that G-CSF therapy is not sufficient for the treatment of neutropenia and neutrophil dysfunction [10]. Recently, it has been proposed that accumulation of 1,5-anhydroglucitol-6-phosphate (1,5-AG6P), a structural analog of G6P and newly discovered substrate for G6PT and G6Pase-β, strongly inhibits the activity of hexokinase in GSD-Ib patients, thereby blocking the first step of glycolysis [11]. This finding led to the observation that administration of a 1,5-AG6P-lowering drug, empagliflozin, treats neutrophil dysfunction in GSD-Ib patients, but neutropenia was not cured in all patients [12]. Therefore, a molecular mechanism underlying neutrophil maturation arrest in GSD-Ib is further required.

Differentiation of neutrophils occurs in the BM and produces more than 1×10^{11} neutrophils every day. In the process of neutrophil differentiation, myeloblasts are the first recognizable myeloid precursor cells. They terminally differentiate into mature neutrophils through morphologically different stages of promyelocytes, myelocytes, metamyelocytes, and band cells [13]. Neutrophils are known to mainly depend on glycolysis; however, several lines of evidence have identified the importance of fatty acid metabolism, the tricarboxylic acid cycle, and mitochondrial respiration during neutrophil development and maturation [14–16]. In particular, it has been observed that autophagy-mediated lipid droplet degradation generates free fatty acids that fuel oxidative phosphorylation (OXPHOS) and provide energy for metabolic reprogramming during neutrophil differentiation, especially in the early developmental stage of myeloblasts and myelocytes [14].

In this regard, we hypothesized that G6PT deficiency could alter the lipid metabolism of myeloid progenitor cells, consequently affecting neutrophil differentiation. We showed that *G6pt*$^{-/-}$ mice exhibited neutropenia and neutrophil maturation arrest in the BM. To provide an insight into the function of G6PT in myeloid progenitor cells, we created G6PT-knockout human promyelocyte HL-60s using the CRISPR/Cas9 and tested their differentiation into neutrophils in vitro. We noted impaired neutrophil differentiation in *G6PT*$^{-/-}$ HL-60s and found that this phenotype is associated with downregulation of nuclear peroxisome proliferator-activated receptor-γ (PPARγ) transcriptional activity and abnormal lipid metabolism. Therefore, we suggest that G6PT plays an essential role in neutrophil maturation through PPARγ regulation.

Materials and methods

Animals

All animal studies were performed in accordance with the guidelines and approval of the Institutional Animal Care and Use Committee of the University of Connecticut Health Center (IACUC protocol number: TE-102122-1022). All mice were maintained in a pathogen-free animal facility at 22 to 24 °C under a 12-h:12-h light–dark cycle in individually ventilated caging systems. Standard rodent chow (Envigo, Madison, WI) and water were provided ad libitum. The *G6pt*$^{-/-}$ mice were obtained from Dr. Janice Chou's laboratory at National Institute of Child Health and Human Development (NICHD), and the *G6pt*$^{-/-}$ mouse model mimics all known defects of the human GSD-Ib and has been used for the model to investigate the pathogenesis of GSD-Ib in several studies [17–19]. Due to the severely low survival rate of *G6pt*$^{-/-}$ mice even with glucose supplement, all *G6pt*$^{-/-}$ mice used in this study were received a recombinant adeno-associated virus serotype 8 (rAAV8) vector carrying human G6PT (hG6PT) neonatally and at age 4 weeks [19]. This liver-directed AAV vector restores the hepatic symptoms of *G6pt*$^{-/-}$ mice including hypoglycemia that enables the treated *G6pt*$^{-/-}$ mice survive, but neutropenia and neutrophil dysfunctions were remained uncured [19]. The AAV-treated *G6pt*$^{-/-}$ mice maintained until age 5–12 weeks to be sacrificed and used for neutrophil analyses.

Cell culture and neutrophil differentiation

The human promyelocytic cell line HL-60 was obtained from ATCC (American Type Culture Collection; ATCC-CCL-240). Cells were grown in RPMI-1640 (HyClone,

Logan, USA) supplemented with 10% heat-inactivated fetal bovine serum (Access Biologicals LLC, Vista, USA) and 1% penicillin/streptomycin (HyClone) at 37 °C in an atmosphere with 5% CO_2. The cultures were at densities between 1×10^5 and 1×10^6 viable cells/mL for constant exponential growth.

For neutrophil differentiation, the cells were cultured to 3×10^5 cells/mL with 1.25% dimethyl sulfoxide (DMSO; Sigma-Aldrich, Saint Louis, MO, USA) and 1 μM all-trans retinoic acid (ATRA; Sigma-Aldrich) treatment.

Flow cytometry analysis

Mouse peripheral blood and BM cells were treated with ammonium-chloride-potassium (ACK) lysis buffer (Thermo Scientific, Waltham, USA). The resulting leukocytes were stained with a monoclonal antibody 1A8-Ly6G also known as Gr-1 which is conjugated with phycoerythrin (PE) (1:50, Cat #12-9668-82, eBioscience, San Diego, USA), peridinin-chlorophyll-protein-cyanine5.5 (PerCP-Cy5.5)-conjugated integrin alpha M (CD11b) antibody (1:50, Cat #45-0112-82, eBioscience), Alexa Fluor® 488-conjugated G-CSF receptor (G-CSFR) antibody (1:20, Cat #FAB60391V, R&D Systems, Minneapolis, USA), and Alexa Fluor® 405-conjugated C-X-C chemokine receptor type 4 (CXCR4) antibody (1:20, Cat #FAB21651RV, R&D Systems) for 20 min at 4 °C in the dark. Cells were analyzed with an Attune NxT Flow Cytometer (Beckman Coulter, Miami, USA).

Neutrophil differentiation of HL-60s was evaluated in terms of expression of CD71-PE (1:50, Cat #555537, BD Biosciences, Franklin Lakes, USA), CD11b-fluorescein isothiocyanate (FITC, 1:50, Cat #301330, BioLegend, Sandiego USA), and CD38-PE-Cy5 (1:50, Cat #303508, BD Biosciences). The cells were stained for 20 min at 4 °C in the dark with antibodies, and flow cytometry was performed using a Guava® EasyCyte™ system (Millipore, Burlington, USA). The data were analyzed using FlowJo v7.0.

Isolation of murine BM neutrophils and their precursors

Using a mouse neutrophil isolation kit (Miltenyi Biotec, Bergisch Gladbach, Germany), we isolated BM-derived neutrophils and their precursors from the femurs and tibias of mice at the age of 7–11 weeks. The procedure was performed as described previously [9]. In short, we removed erythrocytes from isolated BM cells using ACK lysing buffer (Thermo Scientific), and up to 1×10^8 cells were resuspended in PBS (pH 7.2) supplemented with 0.5% bovine serum albumin and 2 mM EDTA. To deplete non-neutrophil lineage cells, 50 μL of Neutrophil Biotin-Antibody Cocktail (Miltenyi Biotec) was mixed with 5×10^7 cells and incubated at 4 °C for 10 min. After washing with buffer, the samples were mixed with 100 μL of Anti-Biotin Microbeads per 5×10^7 cells and incubated at 4 °C for 15 min. Labeled neutrophils and neutrophil precursors were collected using an MACS® column (Miltenyi Biotec). The morphology of isolated cells was examined on Hema-3-stained (Thermo Scientific) cytospin slides.

Immunofluorescence microscopy

To investigate the lipid droplets, differentiated HL-60s were plated onto glass slides using Cytospin™ 4 Cytocentrifuge (Thermo Scientific) and stained with 1 μg/mL BODIPY 493/503 (Invitrogen, Carlsbad, USA) and 4′,6-diamidino-2-phenylindole (DAPI). The slides were imaged using an EVOS5000 system (Invitrogen).

To examine the localization of PPARγ, cells were cytospined and fixed in paraformaldehyde as described previously [7]. Cells were then permeabilized in 1.25% Triton™ X-100 and incubated with PPARγ antibody (1:100, Cat #sc-7273, Santa Cruz Biotechnology, Dallas, USA) and appropriate immunoglobulin G antibody conjugated with Alexa Fluor® 594 (Invitrogen). Cells were visualized using a Zeiss LSM700 confocal microscope equipped with 40×/1.3 numeric aperture oil objectives (Carl Zeiss Microimaging, Oberkochen, Germany).

PPARγ activity in vitro assay

PPARγ activity was measured using a PPARγ transcription factor assay kit (Abcam, Cambridge, UK) and Nuclear Extraction Kit (Abcam), following the manufacturer's instructions. PPARγ activity was measured at 450 nm using an absorbance microplate reader, Sunrise™ (Tecan, Zürich, Switzerland), followed by incubation with PPARγ primary antibody and secondary antibody conjugated to horseradish peroxidase.

Western blotting and quantitative real-time reverse transcription-polymerase chain reaction analysis

Western blot analysis was conducted as described previously [20]. Briefly, cells were lysed with EzRIPA lysis buffer supplemented with protease/phosphatase inhibitors (ATTO, Tokyo, Japan). Thirty micrograms of protein were separated by SDS-PAGE and transferred onto PVDF membrane (Millipore), followed by blocking with 5% skim milk in PBS containing 0.3% Tween 20. The membranes were probed with following primary antibodies: The mouse monoclonal antibodies against glyceraldehyde-3-phosphate dehydrogenase (GAPDH; Cat #sc-365062, Santa Cruz Biotechnology) and peroxisome proliferator-activated receptor g (PPARγ; Cat #sc-7273, Santa Cruz Biotechnology); the rabbit polyclonal antibodies against poly (ADP-ribose) polymerase (PARP; Cat #9542S, Cell Signaling, Danvers, USA), PPARγ

(Cat #sc-7196, Santa Cruz Biotechnology), PPARα (Cat #sc-9000, Santa Cruz Biotechnology), PU.1 (Cat #sc-352, Santa Cruz Biotechnology), NAD-dependent protein deacetylase sirtuin 1 (SIRT1; Cat #07-131, Millipore), and total and phosphorylated extracellular signal-regulated kinase 1/2 (ERK1/2; Cat #4695S, and pERK1/2; Cat #4370S, Cell Signaling). All primary antibodies were incubated at a concentration of 1–5 µg depending on antibodies at 4 °C overnight. After incubation with appropriate secondary antibodies at a concentration of 1 µg at room temperature for 1 h, the membranes were scanned with ImageQuant™ Las4000 (Danaher, Washington, USA). Protein expression was quantified by means of densitometry analysis using ImageJ software v1.50 (National Institutes of Health).

Total RNA was extracted from HL-60s using the TRIzol® Reagent (Invitrogen). Briefly, 5–10 × 10^5 cells were resuspended in 0.5 mL of TRIzol and incubated at room temperature for 15 min, followed by centrifugation at 18,500×*g*. The aqueous phase including mRNA was precipitated with isopropanol. One thousand microgram of mRNA was used to synthesize cDNA using the ReverTra Ace™ qPCR RT Kit (Toyobo, Osaka, Japan) according to the manufacturer instructions. Quantitative real-time reverse transcription-polymerase chain reaction (qRT-PCR) analysis to determine mRNA expression was conducted with an AriaMx Real-Time PCR System (Agilent Technologies, Santa Clara, USA) and was normalized to 18S rRNA. The sequences of each primer pair are shown in Supplementary Table 1.

Real-time cell metabolism assay

The oxygen consumption rate (OCR) and extracellular acidification rate (ECAR) were determined using the Seahorse XFp analyzer (Agilent Technologies), as described by Steven Messina-Graham et al. [21]. Differentiated HL-60s (live 2.5 × 10^5) were plated using Cell-Tak™ (Corning, Corning, NY, USA). For measuring the OCR, 5 µM oligomycin, 0.75 µM carbonyl cyanide-*p*-trifluoromethoxyphenylhydrazone (FCCP), and 1.5 µM Rotenone/Antimycin A were injected in the XFp Analyzer. To measure the ECAR, 10 mM glucose, 5 µM oligomycin, and 50 µM 2-Deoxy-D-glucose were added. Cellular respiration and glycolytic flux were quantified by the OCR (pmol/min) and ECAR (mpH/min), respectively.

Statistical analysis

To ensure the reliability of data, all experiments were performed as independent experiments with three replicates and representative results are shown in figures. For statistical analysis, data have been represented as mean ± SEM and were assessed using Mann–Whitney *U* test using with Prism software 5 (GraphPad Software Inc., CA, USA). Values were considered statistically significant at $*P < 0.05$ and $**P < 0.01$.

Results

G6pt$^{-/-}$ mice exhibit neutropenia and abnormal expression of G-CSFR and CXCR4 in blood

G6pt$^{-/-}$ mice suffer from frequent hypoglycemic seizures and a low survival rate without daily glucose therapy [17]. To increase their survival, *G6pt*$^{-/-}$ mice received rAAV8-hG6PT as previously described [9]. The introduced G6PT transgene induces only transient expression of G6PT in the BM, because the rAAV8-hG6PT vector primarily targeted the liver [19, 22]. Consequently, rAAV8-hG6PT could not correct the neutropenia in *G6pt*$^{-/-}$ mice, and the levels of total neutrophils (CD11b$^+$Gr-1$^+$) in the erythrocyte-depleted blood leukocytes were analyzed using flow cytometry. *G6pt*$^{-/-}$ mice exhibited severe neutropenia, with a significantly lower frequency of CD11b$^+$Gr-1$^+$ neutrophils (by 25.5%) in the peripheral blood, as compared to that in the control littermates (Fig. 1a). Neutropenia in the peripheral blood of *G6pt*$^{-/-}$ mice was also confirmed by nuclear morphologic analysis of Hema-3-stained cytospin slides (Fig. 1b).

GSD-Ib patients showing neutropenia normally receive G-CSF therapy to increase their absolute neutrophil counts. The interesting thing is that they show increased plasma G-CSF levels even before receiving G-CSF therapy; however, the underlying cause why they do not respond to increased G-CSF is still not understood [17]. Also, it was reported that increased chemokine receptor CXCR4-mediated bone marrow retention mechanism might contribute to neutropenia [23]. In this point of view, we compared the expression of G-CSF receptor (G-CSFR) and chemokine receptor CXCR4 in CD11b$^+$Gr-1$^+$ neutrophils. As a result, there was a significant decrease in G-CSFR expression, while CXCR4 expression increased 5.8-fold in *G6pt*$^{-/-}$ mice, as compared to that in control mice (Fig. 1c, d and Fig. S1a).

Impaired neutrophil differentiation in the BM of *G6pt*$^{-/-}$ mice

G6pt $^{-/-}$ mice showed significantly decreased neutrophil population in the BM compared with that in control mice (53.0% *vs.* 19.2% CD11b$^+$Gr-1$^+$ cells in the BM cells) (Fig. 2a). In this population, mature (CD11b$^+$Gr-1$^+$) neutrophils were also reduced to 36.3% in *G6pt*$^{-/-}$ mice, as compared to that in control mice. Furthermore, immature myeloid precursor cells (CD11b$^-$Gr-1$^+$) accumulated 2.4-fold higher in *G6pt*$^{-/-}$ mice than that in control mice,

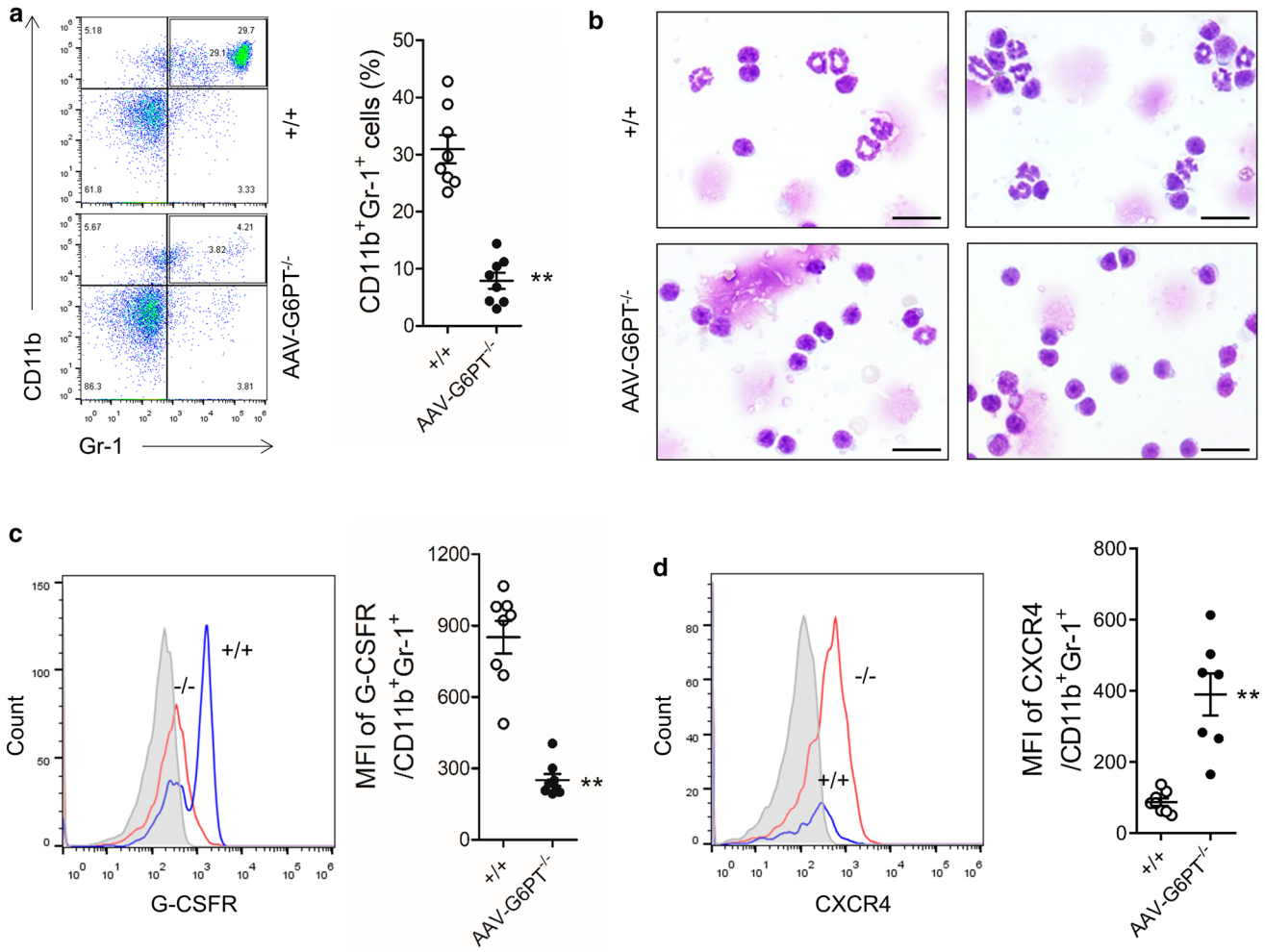

Fig. 1 Neutropenia and abnormal G-CSFR and CXCR4 expression in the peripheral blood of *G6pt*$^{-/-}$ mice. **a** Representative flow cytometry data (left) and frequency of CD11b^{+}Gr-1^{+} neutrophils in the blood of control (WT) and *G6pt*$^{-/-}$ mice. **b** Representative Hema-3-stained cytospins of peripheral blood neutrophils (bar = 20 µm). **c** Representative flow cytometry analysis and mean fluorescence intensity (MFI) of granulocyte-colony stimulating factor receptor (G-CSFR) on CD11b^{+}Gr-1^{+} cells. **d** Representative flow cytometry analysis and MFI of C-X-C chemokine receptor type 4 (CXCR4) on CD11b^{+}Gr-1^{+} cells. Data have been represented as mean ± SEM ($n = 8$ per genotype) and statistical significance was determined by two-tailed Mann–Whitney *U* test. ** $P < 0.01$

accounting for 50.5% of total Gr-1^{+} cells in the BM, while control mice had only 12.8%.

Expression of G-CSFR and CXCR4 in Gr-1^{+} neutrophil lineage cells was also examined in the BM of *G6pt*$^{-/-}$ mice. G-CSFR expression of Gr-1^{+} cells was not significantly different between *G6pt*$^{-/-}$ and control mice. However, the expression of CXCR4 increased by approximately 4.7-fold in *G6pt*$^{-/-}$ mice compared with that in control mice (Fig. 2b, c and Fig. S1b). Accumulation of immature myeloid precursor cells in the BM of *G6pt*$^{-/-}$ mice was confirmed by Hema-3-stained cytospin slides (Fig. 2d). These results indicated that G6PT deficiency significantly inhibits the ability of myeloid progenitor cells to differentiate into neutrophils.

Decreased neutrophil differentiation of *G6PT*$^{-/-}$ HL-60s

Since *G6pt*$^{-/-}$ mice are rare, to further pursue mechanistic studies, we generated a *G6PT*$^{-/-}$ clone via CRISPR/Cas9-mediated gene editing of the in vitro human promyelocyte line HL-60s (Fig. S2a–c). First, we examined cell growth by counting cells at the indicated time-points to investigate the proliferative activity of *G6PT*$^{-/-}$ HL-60s (Fig. 3a). *G6PT*$^{-/-}$ HL-60s exhibited increased cell proliferation, as compared to control HL-60s in the absence of ATRA and DMSO. *G6PT*$^{-/-}$ HL-60s also showed increased cell numbers up to 96 h after induction, while control HL-60s showed a decrease in cell number after 48 h, as neutrophil

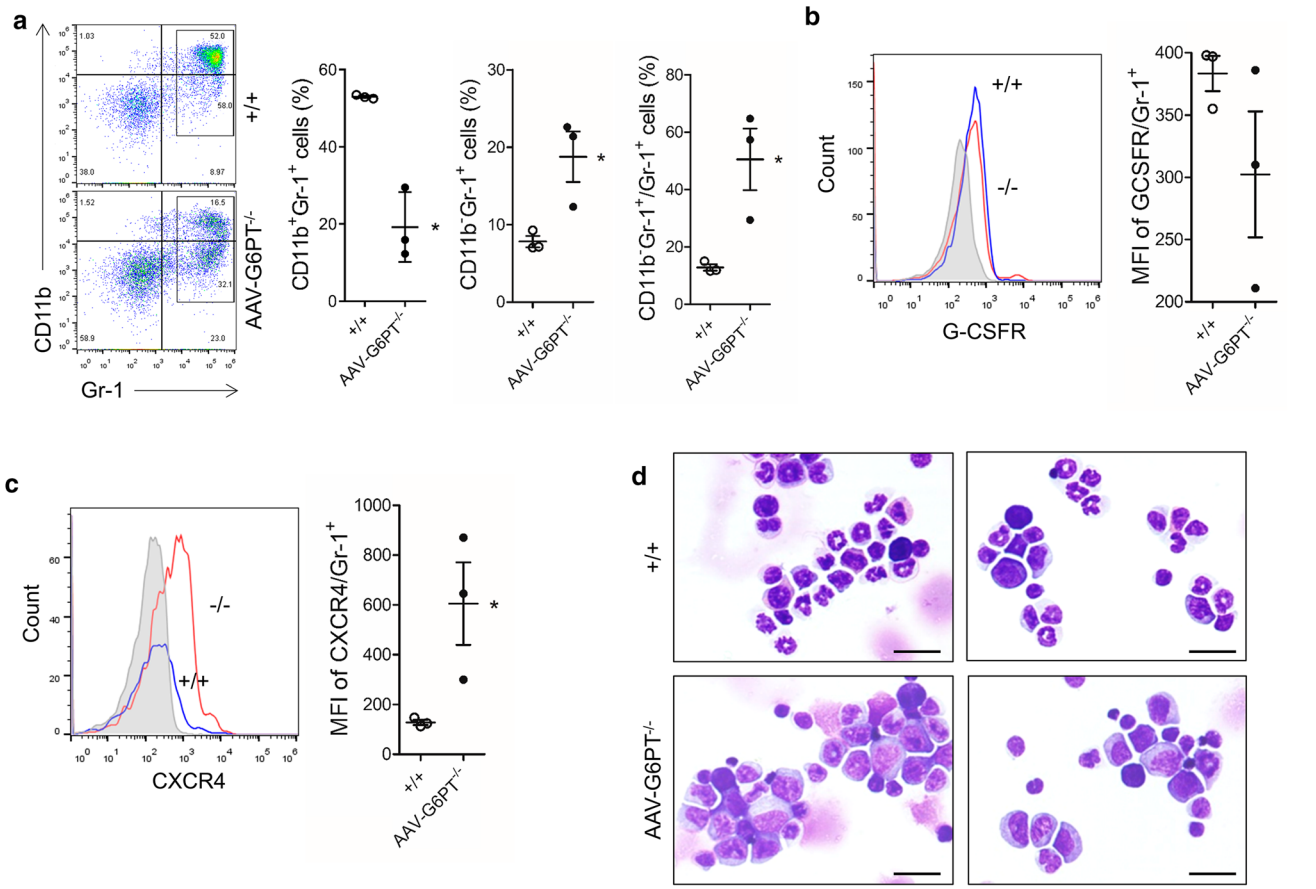

Fig. 2 Accumulation of neutrophil precursor cells in the bone marrow of *G6pt*$^{-/-}$ mice. **a** Representative flow cytometry data (left) and frequency of mature (CD11b^{+}Gr-1^{+}), immature neutrophil precursors (CD11b^{-}Gr-1^{+}), and ratio of immature (CD11b^{-}Gr-1^{+}/Gr-1^{+}) cells in the bone marrow of control (WT) and *G6pt*$^{-/-}$ mice. **b** Representative flow cytometry analysis and mean fluorescence intensity (MFI) of granulocyte-colony-stimulating factor receptor (G-CSFR) on Gr-1^{+} cells. **c** Representative flow cytometry analysis and MFI of C-X-C chemokine receptor type 4 (CXCR4) on Gr-1^{+} cells. **d** Representative Hema-3-stained cytospins of isolated bone marrow neutrophil lineage cells (bar = 20 µm). Data have been represented as mean ± SEM ($n = 3$ per genotype) and statistical significance was determined by two-tailed Mann–Whitney *U* test. * $P < 0.05$

differentiation proceeded. Next, we examined the neutrophil differentiation of *G6PT*$^{-/-}$ HL-60s to study the effect of G6PT deficiency. Neutrophil differentiation of HL-60s was analyzed by CD71 (undifferentiated HL-60 marker), CD38 (early differentiation marker), and CD11b (late differentiation marker) expression using flow cytometry and nuclear morphological analysis of Hema-3-stained cytospin slides [24]. The frequency of CD38^{+}CD71^{-} cells and mean fluorescence intensity (MFI) of CD38 expression was significantly lower in *G6PT*$^{-/-}$ HL-60s than in control HL-60s (Fig. 3b). The frequency of CD11b^{+}CD71^{-} cells was also significantly lower in *G6PT*$^{-/-}$ HL-60s, as compared to that in control HL-60s (Fig. 3c). Consistently, highly differentiated cells were not observed in *G6PT*$^{-/-}$ HL-60s (Fig. 3d). These results indicated that G6PT deficiency results in maturation arrest from the early stages of neutrophil differentiation.

Interestingly, *G6PT*$^{-/-}$ HL-60s showed a dramatic decrease in cell number 120 h after induction (Fig. 3a). Therefore, we assessed apoptosis of differentiated HL-60s using two apoptosis markers; externalization of phosphatidylserine on the plasma membrane and expression of cleaved PARP. As HL-60s differentiate into neutrophils, control HL-60s showed continuously increasing rates of apoptosis, while apoptosis rates of *G6PT*$^{-/-}$ HL-60s were significantly low until 72 h and they increased after 96 h (Fig. 3e and S3a). On the other hand, cleaved PARP expression was upregulated in *G6PT*$^{-/-}$ HL-60s from 72 h after induction (Fig. S3b), suggesting that cleaved PARP-mediated apoptosis would contribute to an increase of apoptosis in *G6PT*$^{-/-}$ HL-60 from 96 to 120 h (Fig. 3a).

GSD-Ib patients suffer from hypoglycemia; therefore, the amount of glucose available for the myeloid progenitor cells in the BM of the patients would be lesser than the amount

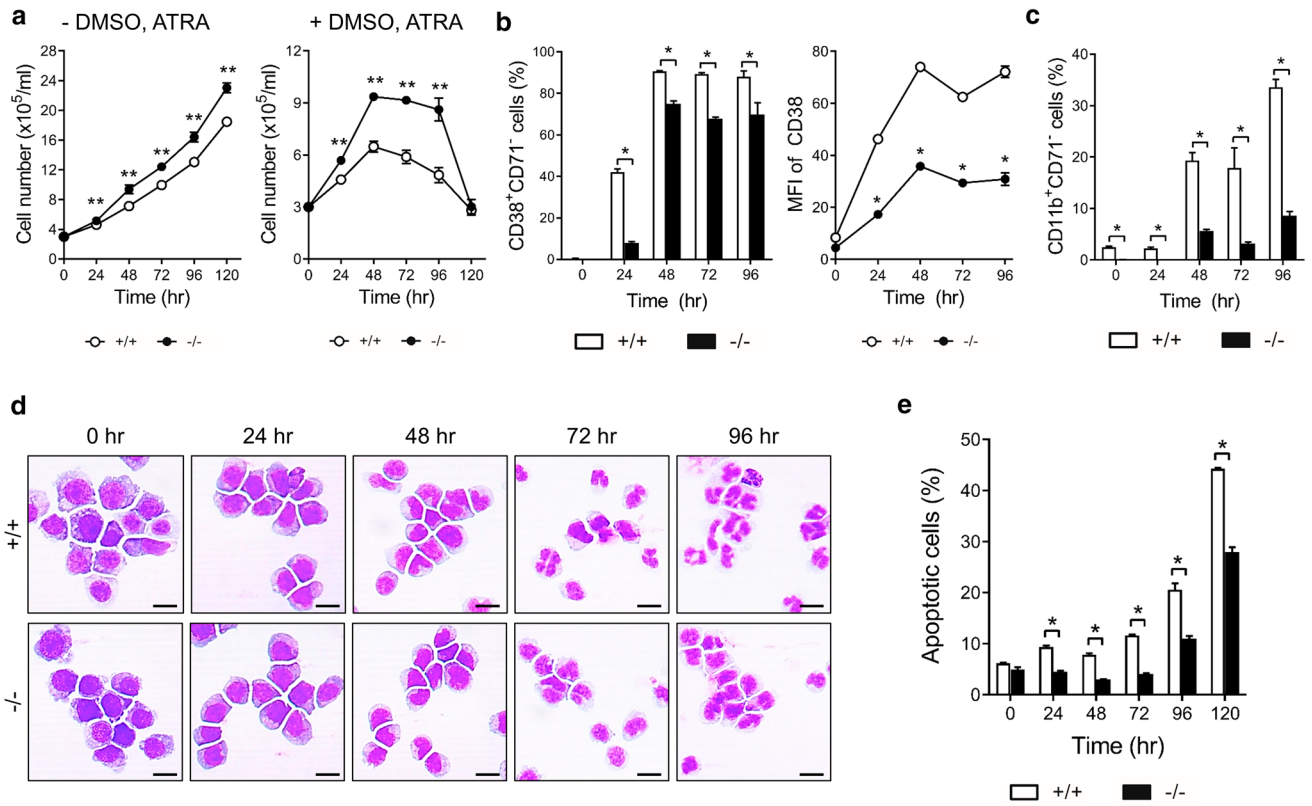

Fig. 3 Impaired neutrophil differentiation in *G6PT*$^{-/-}$ human promyelocyte HL-60s. **a** Growth curve of control and *G6PT*$^{-/-}$ HL-60s for the indicated times in the normal (left) and neutrophil differentiation-induced (right) conditions ($n=9$). **b** Frequency of $CD38^{+}CD71^{-}$ cells and mean fluorescence intensity (MFI) of CD38 expression for the indicated time after differentiation induction ($n=3$). **c** Frequency of $CD11b^{+}CD71^{-}$ cells at the indicated time ($n=3$). **d** Representative Hema-3-stained cytospins of dimethyl sulfoxide (DMSO) and all-trans retinoic acid (ATRA)-induced control and *G6PT*$^{-/-}$ HL-60s (bar = 10 μm, $n=3$). **e** Frequency of annexin V-positive apoptotic cells at the indicated time. Data have been represented as mean ± SEM ($n=3$) and statistical significance was determined by two-tailed Mann–Whitney *U* test. $^{*}P<0.05$, $^{**}P<0.01$

present in the culture condition (11 mM glucose). For this reason, we tested neutrophil differentiation of *G6PT*$^{-/-}$ HL-60s depending on the glucose concentration in the media. While control HL-60s exhibited growth arrest from 48 h after induction in all conditions, *G6PT*$^{-/-}$ HL-60s showed decreased proliferation depending on the glucose concentrations and did not show growth arrest (Fig. S4a, b). When we investigated neutrophil differentiation markers under these conditions, the MFI of CD38 expression and frequency of $CD11b^{+}$ cells were significantly reduced in *G6PT*$^{-/-}$ HL-60 cells, regardless of the glucose concentration (Fig. S4c). Impaired neutrophil maturation of *G6PT*$^{-/-}$ HL-60s was also confirmed by assessing the Hema-3-stained cytospin slides (Fig. S4d). Along with these results, *G6PT*$^{-/-}$ HL-60s exhibited glucose susceptibility compared to control HL-60s, when we treated 0.5 mM 2-deoxy-D-glucose (2-DG) that is a non-metabolizable glucose analog (Fig. S4e). Of note, inhibition of glycolysis by 2-DG slightly increased neutrophil differentiation in both control and *G6PT*$^{-/-}$ HL-60s (Fig. S4f, g). These results suggested that glucose might affect the proliferation, but not maturation, during neutrophil differentiation of *G6PT*$^{-/-}$ HL-60s.

Abnormal lipid metabolism and reduced nuclear PPARγ activity of *G6PT*$^{-/-}$ HL-60s

Recently, the FAO and OXPHOS/mitochondrial respiration in neutrophil differentiation has been considered as a major metabolic pathway [25]. Therefore, we examined lipid droplets during neutrophil differentiation to investigate the molecular mechanisms governing impaired neutrophil differentiation in *G6PT*$^{-/-}$ HL-60s. There was a significant decrease in the amount of BODIPY-stained lipid droplets in undifferentiated *G6PT*$^{-/-}$ HL-60s, as compared to that in the control HL-60s (Fig. 4a). As differentiation proceeded, the size of lipid droplets became smaller and they almost disappeared at 48 h after induction in control HL-60s. However, *G6PT*$^{-/-}$ HL-60s showed very few lipid droplets and did not accumulate as much as those in control HL-60s for up to 96 h.

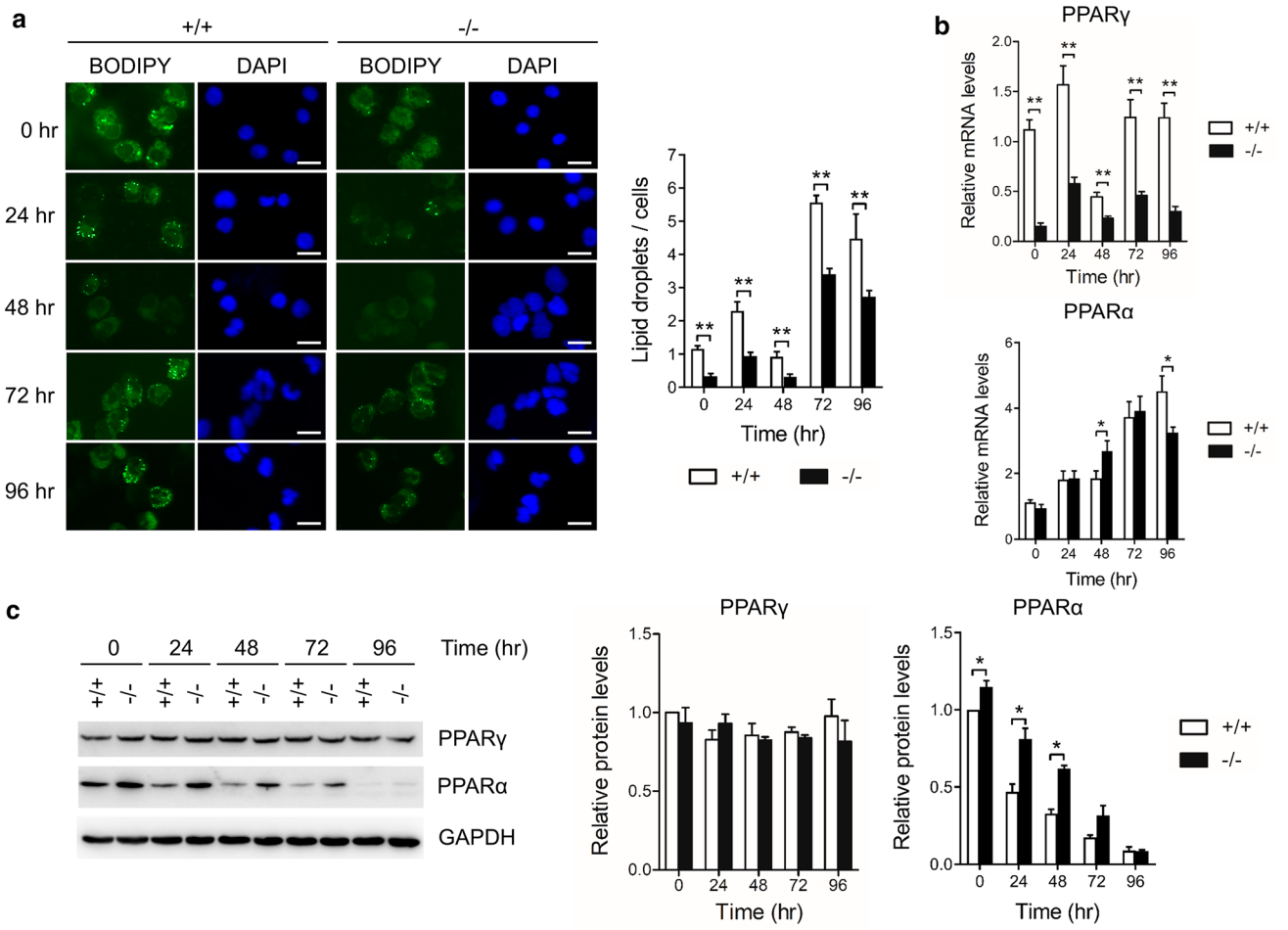

Fig. 4 Aberrant regulation of lipid metabolism by PPARγ and PPARα in *G6PT*$^{-/-}$ HL-60s. **a** Representative images of BODIPY-stained lipid droplets of control and *G6PT*$^{-/-}$ HL-60s (bar = 10 μm) after dimethyl sulfoxide (DMSO) and all-trans retinoic acid (ATRA) induction (left) and quantification of lipid droplets (right) ($n = 3$). **b** mRNA levels of peroxisome proliferator-activated receptor-γ (PPARγ) and peroxisome proliferator-activated receptor-α (PPARα) ($n = 9$). **c** Western blot analysis and quantification of PPARγ and PPARα ($n = 3$). Data have been represented as mean ± SEM and statistical significance was determined by two-tailed Mann–Whitney *U* test. *$P < 0.05$, **$P < 0.01$

We then investigated the expression of PPARγ and PPARα, which regulate lipid metabolism and genes related to cell differentiation [26]. As shown in Fig. 4b, PPARγ mRNA expression was downregulated in *G6PT*$^{-/-}$ HL-60s, while PPARα mRNA expression was not significantly different in both control and *G6PT*$^{-/-}$ HL-60s during differentiation. On the other hand, western blot analysis showed that expression of PPARα was upregulated in *G6PT*$^{-/-}$ HL-60s, whereas PPARγ expression did not change during differentiation in both control and *G6PT*$^{-/-}$ HL-60s (Fig. 4c).

Even though PPARγ protein expression in both control and *G6PT*$^{-/-}$ HL-60s was similar, PPARγ mRNA expression was significantly lower in *G6PT*$^{-/-}$ HL-60s. In addition, PPARγ is known to induce differentiation by regulating transcription in the nucleus, so we examined the localization and activity of PPARγ. Confocal microscopic analysis confirmed downregulation of PPARγ nuclear localization and it was mainly located in the cytoplasm of *G6PT*$^{-/-}$ HL-60s, as compared to that in control HL-60s (Fig. 5a and S5a). Consistent with this, we found that *G6PT*$^{-/-}$ HL-60s showed a decrease in PPARγ activity in the nuclear fraction (Fig. 5b).

To validate the results of the PPARγ localization and activity test in *G6PT*$^{-/-}$ HL60s, we examined the expression of genes highly regulated by PPARγ. These genes include p21 and CD38, which control cell cycle arrest and early stages of neutrophil differentiation, and CD36, ATP-binding cassette subfamily G member 1 (ABCG1), and acyl-CoA thioesterase 2 (ACOT2), which are involved in the regulation of lipid metabolism [24, 27–29]. Consequently, the expression of all these genes (p21, CD38, CD36, ABCG1, and ACOT2) were downregulated in *G6PT*$^{-/-}$ HL-60s (Figs. 5c, 3b). Taken together, these results indicated that

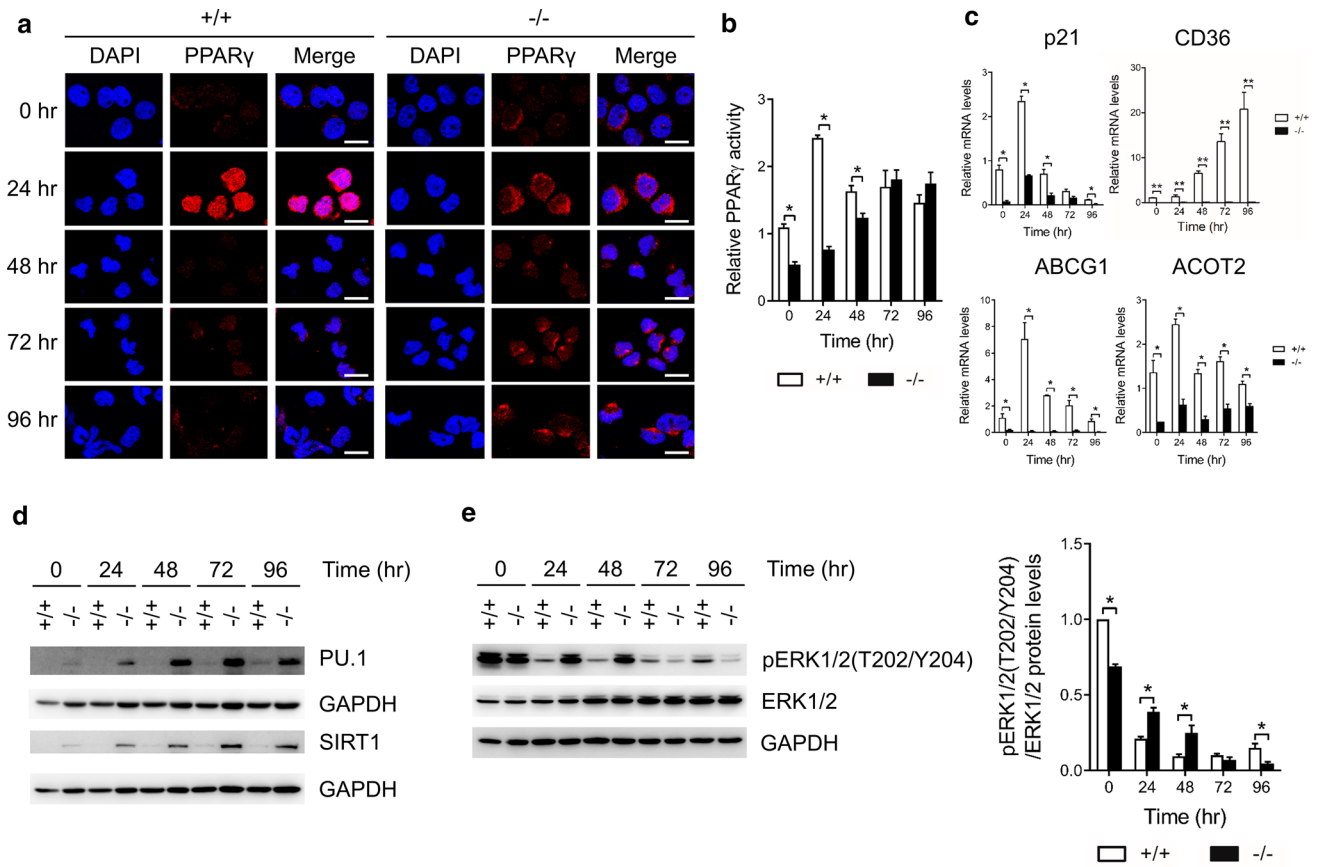

Fig. 5 Decreased nuclear localization and transcriptional activity of PPARγ in *G6PT*$^{-/-}$ HL-60s. **a** Confocal analysis of peroxisome proliferator-activated receptor-γ (PPARγ, red fluorescence) and DAPI staining (blue fluorescence) at original magnification of 400× (bar = 10 µm, $n = 3$). **b** Relative fold change of nuclear PPARγ activity ($n = 3$). **c** mRNA levels of p21, CD36, ATP-binding cassette subfamily G member 1 (ABCG1), and acyl-CoA thioesterase 2 (ACOT2) ($n = 3$). **d** Protein levels of PU.1 and NAD-dependent protein deacetylase sirtuin 1 (SIRT1) ($n = 3$). **e** Western blot analyses of phosphorylated and total extracellular signal-regulated kinase 1/2 (ERK1/2). The ratio of the phosphorylated form to the total form is shown on the right ($n = 3$). Data have been represented as mean ± SEM and statistical significance was determined by two-tailed Mann–Whitney *U* test. *$P < 0.05$, **$P < 0.01$

G6PT deficiency inhibits the nuclear transcriptional activity of PPARγ, thereby impairing the maturation of neutrophils.

Aberrant PU.1 and SIRT1 expression and ERK1/2 signaling in *G6PT*$^{-/-}$ HL-60s

Nuclear localization and transcriptional activity of PPARγ are regulated by other transcription factors and several post-translational modifications such as deacetylation and phosphorylation [30, 31]. For example, overexpression of PU.1 is related to inhibition of genomic binding of PPARγ and deacetylation of PPARγ by sirtuin 1 (SIRT1) leads to repression of PPARγ activity, thereby blocking adipogenesis [31, 32]. Also, it was reported that phosphorylation by ERK1/2 leads to repression of PPARγ transactivation, altering affinity for ligands and co-factors [33, 34]. In this view, we further examined PU.1 and SIRT1 protein expression and phosphorylation of ERK1/2 in *G6PT*$^{-/-}$ HL-60s after DMSO and ATRA induction. Western blot analysis showed that protein expression of PU.1 and SIRT1 continuously increased in *G6PT*$^{-/-}$ HL-60s compared to that in control HL-60s (Fig. 5d). In addition, we found that delayed dephosphorylation of ERK1/2 in *G6PT*$^{-/-}$ HL-60s, indicating disturbed nuclear localization of PPARγ (Fig. 5e). These results support our finding that impaired neutrophil differentiation results from reduced nuclear PPARγ activity in *G6PT*$^{-/-}$ HL-60s.

Abnormal metabolic changes in *G6PT*$^{-/-}$ HL-60s during neutrophil differentiation

In neutrophil differentiation, a metabolic shift from glycolysis to FAO and OXPHOS/mitochondrial respiration has been reported [14, 35]. This metabolic change is fueled by the degradation of lipid droplets for FAO and mitochondrial respiration that occurs in the early stage

of differentiation [14]. As the neutrophil progenitor cells become mature, the increase in mitochondrial respiration is reduced again and glycolysis increases [35]. Therefore, we investigated the impact of G6PT deficiency on the metabolic pathway by measuring the OCR and ECAR using the XF analyzer over a period of 72 h after induction. When we measured the OCR, non-mitochondrial respiration was higher in *G6PT*$^{-/-}$ HL-60s than that in control HL-60s (Fig. 6a, b), suggesting insufficient mitochondrial electron transport or oxidative reactions in *G6PT*$^{-/-}$ HL-60s [36]. Furthermore, it was revealed that mitochondrial respiration in *G6PT*$^{-/-}$ HL-60s was delayed, but continuously increased without metabolic changes toward glycolysis. In line with the increase in OCR, glycolysis in both control and *G6PT*$^{-/-}$ HL-60s decreased during neutrophil differentiation; however, control HL-60s showed re-increase of glycolysis at 72 h (Fig. 6c, d). These results suggested that the genetic loss of G6PT induces abnormal metabolic reprogramming, which underlies neutrophil maturation arrest.

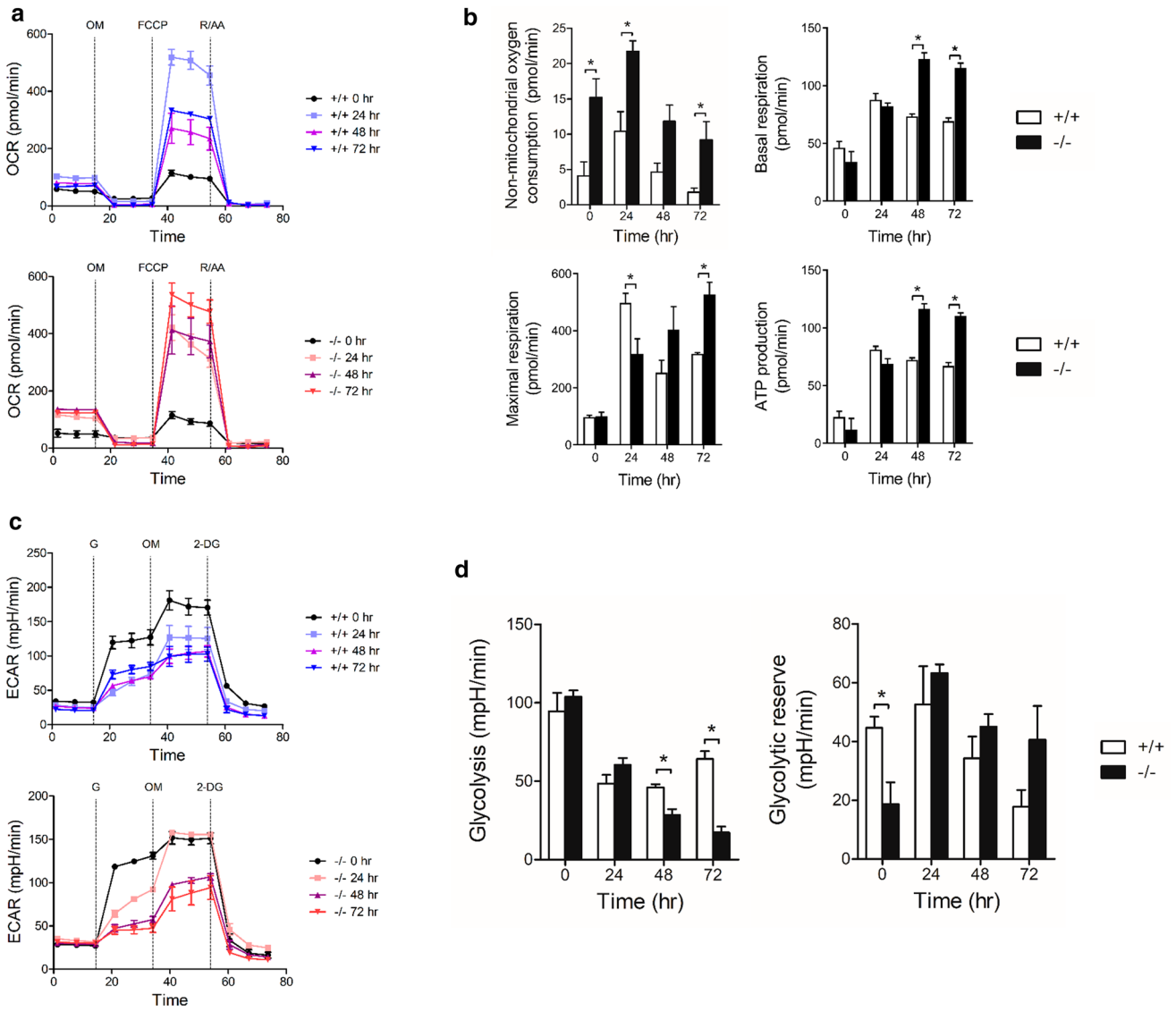

Fig. 6 Measurement of the mitochondrial oxygen consumption rate and extracellular acidification rate of control and *G6PT*$^{-/-}$ HL-60s during neutrophil differentiation. **a** Kinetic profile of oxygen consumption rate (OCR) assay of control and *G6PT*$^{-/-}$ HL-60s. OCR was measured in real time in response to three compounds; oligomycin (OM), FCCP, and rotenone/antimycin A (R/AA) ($n=3$). **b** Individual plots for non-mitochondrial respiration, basal respiration, maximal respiratory capacity, and ATP production. **c** Determination of extracellular acidification rate (ECAR) ($n=3$). **d** Individual plots for glycolysis and glycolytic reserve. Data have been represented as mean ± SEM and statistical significance was determined by two-tailed Mann–Whitney *U* test. *$P<0.05$

Discussion

GSD-Ib is a rare inherited metabolic disorder caused by a deficiency in G6PT, which is ubiquitously expressed and plays a role in maintaining intracellular glucose homeostasis [2]. Consequently, GSD-Ib is characterized by abnormal metabolic phenotypes including hypoglycemia, hepatomegaly, nephromegaly, and abnormal metabolic profile caused by impaired gluconeogenesis and glycogenolysis [37]. GSD-Ib also exhibits neutropenia and neutrophil dysfunction, resulting in recurrent bacterial infections [2]. Previously, it has been reported that neutropenia in GSD-Ib is caused by enhanced neutrophil ER stress and apoptosis [18]. Moreover, impaired neutrophil energy homeostasis and activation of HIF-1αPPARγ signaling are involved partly in neutrophil dysfunction in GSD-Ib [7]. This study observed immature neutrophils in peripheral blood in GSD-Ib patients and raised the possibility that deficiency of G6PT might induce impaired neutrophil differentiation in the BM.

In the present study, we found that immature neutrophils were prominent both in the peripheral blood stream and BM of *G6pt*$^{-/-}$ mice, compared with control mice. In parallel, the expression of CXCR4 on peripheral blood neutrophils was increased. It is known that CXCR4 increases on neutrophils as they ages and become apoptotic [38] and GSD-Ib neutrophils were shown to undergo increased ER stress and enhanced apoptosis [18]. Therefore, increased CXCR4 on peripheral blood and BM neutrophils might in part result from apoptosis. In addition, the expression of CXCR4 is negatively related to neutrophil maturation, and negatively regulates neutrophil release from BM [38, 39]. It is therefore reasonable to speculate that the upregulation of CXCR4 on neutrophils of *G6pt*$^{-/-}$ mice is attributed to prominent immature neutrophils. Decreased egress and aberrant return to the bone marrow due to increased CXCR4 should be further studied.

The G-CSFR is a member of the cytokine receptor superfamily, playing a critical role in neutrophil production, trafficking, and maturation [40, 41]. In this study, the expression of G-CSFR on peripheral neutrophils of *G6pt*$^{-/-}$ mice was significantly decreased, which might result from abundant immature neutrophils. Unlike peripheral neutrophils, the expression of G-CSFR on BM neutrophils was not significantly different between *G6pt*$^{-/-}$ and control mice with big inter-individual variations. The variation could be explained as follows: (i) the percentage of immature neutrophils in Gr-1^{+} cells in BM was ranged from 30 to 67% which might affect the G-CSFR expression; (ii) Chen and colleagues reported that plasma concentrations of G-CSF are fluctuated depending on ages and severity of neutropenia [17]. It is reasonable to speculate that the variation of G-CSFR expression on BM neutrophils is in part due to plasma G-CSF concentrations. However, further study should be conducted with a large number of *G6pt*$^{-/-}$ mice.

To investigate the molecular mechanisms governing incomplete neutrophil maturation, we knocked out the human *G6PT* gene in the promyelocyte HL-60 cell line. We found that *G6PT*$^{-/-}$ HL-60s exhibit impaired differentiation into neutrophils (Fig. 7). This aberrant differentiation of *G6PT*$^{-/-}$ HL-60s can be partly attributed to the decreased transcriptional activity of PPARγ and abnormal metabolic reprogramming toward excessive mitochondrial respiration. These results indicated that G6PT plays an essential role in regulating neutrophil differentiation of myeloid progenitor cells.

The loss of G6PT activity resulted in impaired neutrophil differentiation in the HL-60s. The reasons for this result may be associated with altered metabolism of *G6PT*$^{-/-}$ HL-60s, that is, a metabolic imbalance toward incessant mitochondrial respiration, in part supported by increased expression of the lipid metabolism regulator PPARα and decreased lipid droplets. PPARα primarily regulates the expression of genes related to fatty acid oxidation, and its ligand-dependent activation stimulates lipolysis and reduces fat storage [26, 42]. Consistent with the upregulation of PPARα, there was a significant decrease in the number of lipid droplets in *G6PT*$^{-/-}$ HL-60s. This altered metabolism may inhibit neutrophil maturation of *G6PT*$^{-/-}$ HL-60s, since a metabolic switch from OXPHOS to glycolysis, followed by an initial increase in OXPHOS fueled by FAO, is known to occur during neutrophil differentiation [14, 35]. This excessive energy production may cause ATP depletion, thereby leading to increased expression of cleaved PARP.

Another possible explanation for aberrant neutrophil differentiation is reduced nuclear transcriptional regulation of PPARγ in *G6PT*$^{-/-}$ HL-60s (Fig. 5). In contrast to the function of PPARα, PPARγ contributes to energy storage and lipid synthesis and functions as a master regulator of adipocyte differentiation [43]. PPARγ is mainly expressed in white adipose tissue as well as in the liver, intestine, and immune cells [44, 45]. Therefore, the differentiation induction role of PPARγ in other cells has been investigated. In neutrophil differentiation studies, it has been reported that PPARγ is critical for ATRA-induced neutrophil differentiation in HL-60s, regulating cell cycle arrest and receptor signaling [24]. In this study, we found decreased nuclear localization of PPARγ in *G6PT*$^{-/-}$ HL-60s after DMSO and ATRA induction. This was further supported by the fact that there was a reduction in the nuclear PPARγ transcriptional activity in *G6PT*$^{-/-}$ HL-60s and, in turn, a decrease in the mRNA expression of p21, CD36, ABCG1, and ACOT2. In addition, it leads to metabolic imbalance toward continuous

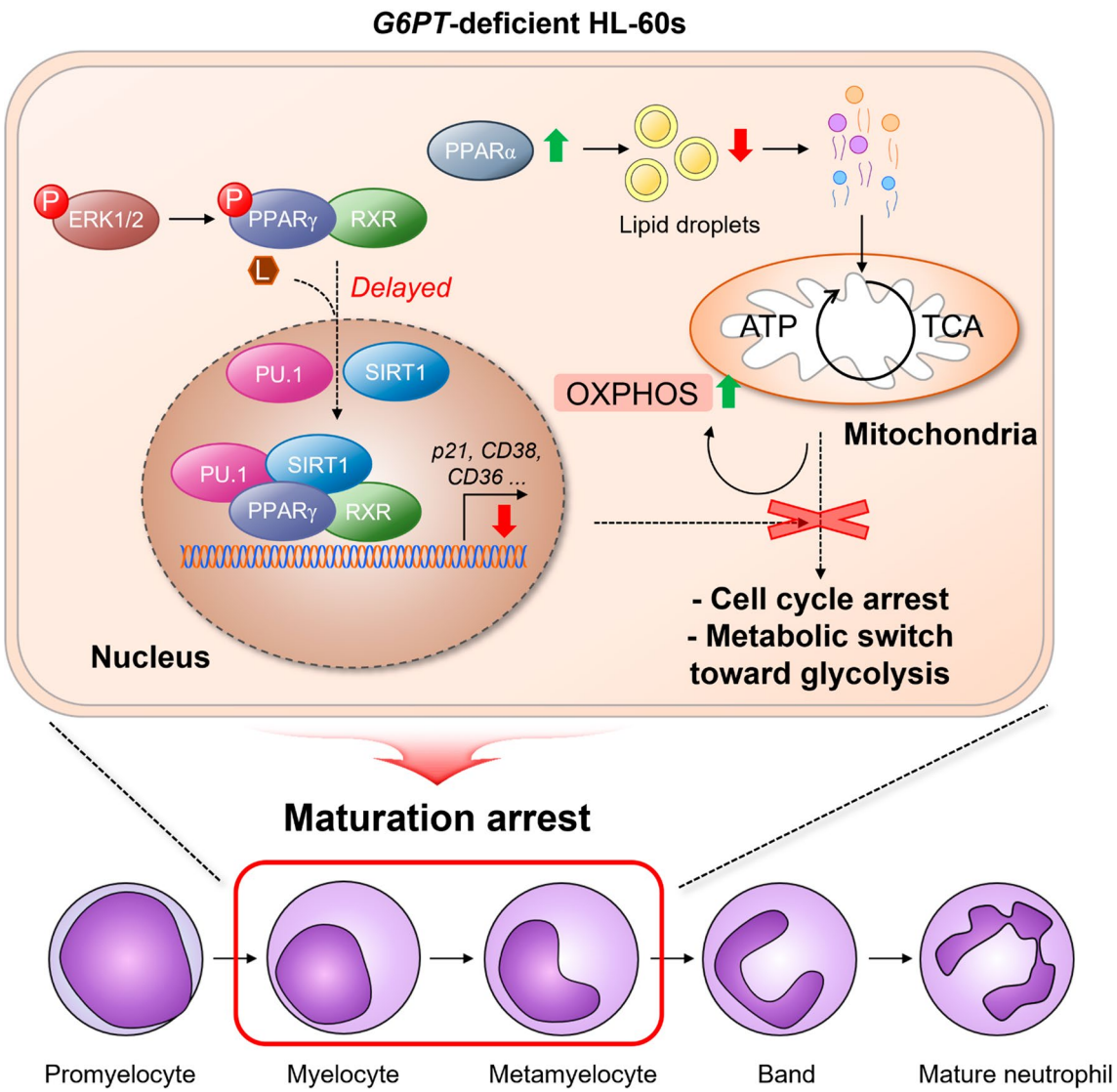

Fig. 7 Proposed mechanisms underlying maturation arrest caused by glucose-6-phosphate transporter (G6PT) deficiency during neutrophil development. G6PT deficiency causes impaired neutrophil differentiation, as compared to that seen in control HL-60s. This phenotype can be explained by two proposed mechanisms. Metabolic reprogramming in *G6PT*$^{-/-}$ HL-60s causes a shift toward excessive mitochondrial oxidative phosphorylation, which is associated with upregulation of peroxisome proliferator-activated receptor-α and reduced accumulation of lipid droplets. In addition, decreased nuclear localization and transcriptional activity of peroxisome proliferator-activated receptor-γ (PPARγ) impair cell cycle arrest and PPARγ-induced transcriptional regulations in *G6PT*$^{-/-}$ HL-60s during neutrophil differentiation

increase of mitochondrial respiration in *G6PT*$^{-/-}$ HL-60s without changes into glycolysis as that in control HL-60s.

The exact mechanism by which G6PT deficiency decreases the transcriptional activity of PPARγ needs to be investigated, but one possible explanation is that increased expression of SIRT1 and PU.1 may repress PPARγ transcriptional activity [31, 32]. Furthermore, upregulated phosphorylation of ERK1/2 can alter the affinity for PPARγ ligands and co-factors, thus repressing the nuclear localization of PPARγ in *G6PT*$^{-/-}$ HL-60s. However, there is still a need to carry out further study in this regard.

Supplementary Information The online version contains supplementary material available at https://doi.org/10.1007/s00018-022-04267-5.

Acknowledgements We thank Dr. Janice Chou at the National Institute of Child Health and Human Development for providing *G6pt*$^{-/-}$ mice and the AAV-gene therapy vector containing human G6PT for this study. We also thank the Global Center for GSD for grant support along with the following GSD-Ib philanthropy funds managed by the University of Connecticut Foundation: The Catherine McMillan Fund, The Jamie Konieczka Fund, The Jonah Pournazarian Fund, The Nina Contreras D'Agosto Fund, and The Sophie LaFreniere GSD-Ib Fund.

Author contributions SWS designed and performed the research, analyzed data, and wrote the paper. YYJ, PTS, and PBC analyzed data and wrote the paper. HSJ and YML designed the research, analyzed data, and wrote the paper.

Funding This work was carried out with the support of the Korea Medical Device Development Fund grant funded by the Korean government (Ministry of Science and ICT, Ministry of Trade, Industry and Energy, Ministry of Health & Welfare, and Ministry of Food and Drug Safety; 202012E04). Additional support was provided by the Basic Science Research Program through the National Research Foundation of Korea (NRF) funded by the Ministry of Education, Science, and Technology (2021R1I1A3056109).

Data availability Data available on request from the authors.

Declarations

Conflict of interest The authors have no relevant financial or non-financial interests to disclose.

Ethics approval All animal studies were conducted under an animal protocol approved by the Institutional Animal Care and Use Committee of the University of Connecticut School of Medicine (IACUC protocol number: TE-102122-1022).

Consent to participate Not applicable.

Consent to publish Not applicable.

References

1. Chou JY, Jun HS, Mansfield BC (2010) Glycogen storage disease type I and G6Pase-beta deficiency: etiology and therapy. Nat Rev Endocrinol 6:676–688. https://doi.org/10.1038/nrendo.2010.189
2. Chou JY, Jun HS, Mansfield BC (2010) Neutropenia in type Ib glycogen storage disease. Curr Opin Hematol 17:36–42. https://doi.org/10.1097/MOH.0b013e328331df85
3. Hiraiwa H, Pan CJ, Lin B, Moses SW, Chou JY (1999) Inactivation of the glucose 6-phosphate transporter causes glycogen storage disease type 1b. J Biol Chem 274:5532–5536. https://doi.org/10.1074/jbc.274.9.5532
4. Chou JY, Matern D, Mansfield BC, Chen YT (2002) Type I glycogen storage diseases: disorders of the glucose-6-phosphatase complex. Curr Mol Med 2:121–143. https://doi.org/10.2174/1566524024605798
5. Visser G, Rake JP, Fernandes J, Labrune P, Leonard JV, Moses S, Ullrich K, Smit GP (2000) Neutropenia, neutrophil dysfunction, and inflammatory bowel disease in glycogen storage disease type Ib: results of the European study on glycogen storage disease type I. J Pediatr 137:187–191. https://doi.org/10.1067/mpd.2000.105232
6. Sim SW, Weinstein DA, Lee YM, Jun HS (2020) Glycogen storage disease type Ib: role of glucose-6-phosphate transporter in cell metabolism and function. FEBS Lett 594:3–18. https://doi.org/10.1002/1873-3468.13666
7. Jun HS, Weinstein DA, Lee YM, Mansfield BC, Chou JY (2014) Molecular mechanisms of neutrophil dysfunction in glycogen storage disease type Ib. Blood 123:2843–2853. https://doi.org/10.1182/blood-2013-05-502435
8. Calderwood S, Kilpatrick L, Douglas SD, Freedman M, Smith-Whitley K, Rolland M, Kurtzberg J (2001) Recombinant human granulocyte colony-stimulating factor therapy for patients with neutropenia and/or neutrophil dysfunction secondary to glycogen storage disease type 1b. Blood 97:376–382. https://doi.org/10.1182/blood.v97.2.376
9. Kim GY, Lee YM, Kwon JH, Jun HS, Chou J (2017) Glycogen storage disease type Ib neutrophils exhibit impaired cell adhesion and migration. Biochem Biophys Res Commun 482:569–574. https://doi.org/10.1016/j.bbrc.2016.11.075
10. Li AM, Thyagu S, Maze D, Schreiber R, Sirrs S, Stockler-Ipsiroglu S, Sutherland H, Vercauteren S, Schultz KR (2018) Prolonged granulocyte colony stimulating factor use in glycogen storage disease type 1b associated with acute myeloid leukemia and with shortened telomere length. Pediatr Hematol Oncol 35:45–51. https://doi.org/10.1080/08880018.2018.1440675
11. Veiga-da-Cunha M, Chevalier N, Stephenne X, Defour JP, Paczia N, Ferster A, Achouri Y, Dewulf JP, Linster CL, Bommer GT, Van Schaftingen E (2019) Failure to eliminate a phosphorylated glucose analog leads to neutropenia in patients with G6PT and G6PC3 deficiency. Proc Natl Acad Sci U S A 116:1241–1250. https://doi.org/10.1073/pnas.1816143116
12. Wortmann SB, Van Hove JLK, Derks TGJ, Chevalier N, Knight V, Koller A, Oussoren E, Mayr JA, van Spronsen FJ, Lagler FB, Gaughan S, Van Schaftingen E, Veiga-da-Cunha M (2020) Treating neutropenia and neutrophil dysfunction in glycogen storage disease type Ib with an SGLT2 inhibitor. Blood 136:1033–1043. https://doi.org/10.1182/blood.2019004465
13. Bainton DF, Ullyot JL, Farquhar MG (1971) The development of neutrophilic polymorphonuclear leukocytes in human bone marrow. J Exp Med 134:907–934
14. Riffelmacher T, Clarke A, Richter FC, Stranks A, Pandey S, Danielli S, Hublitz P, Yu Z, Johnson E, Schwerd T, McCullagh J, Uhlig H, Jacobsen SEW, Simon AK (2017) Autophagy-dependent generation of free fatty acids is critical for normal neutrophil differentiation. Immunity 47:466–480. https://doi.org/10.1016/j.immuni.2017.08.005
15. Six E, Lagresle-Peyrou C, Susini S, De Chappedelaine C, Sigrist N, Sadek H, Chouteau M, Cagnard N, Fontenay M, Hermine O, Chomienne C, Reynier P, Fischer A, Andre-Schmutz I, Gueguen N, Cavazzana M (2015) AK2 deficiency compromises the mitochondrial energy metabolism required for differentiation of human neutrophil and lymphoid lineages. Cell Death Dis 6:e1856. https://doi.org/10.1038/cddis.2015.211
16. Rozman S, Yousefi S, Oberson K, Kaufmann T, Benarafa C, Simon HU (2015) The generation of neutrophils in the bone marrow is controlled by autophagy. Cell Death Differ 22:445–456. https://doi.org/10.1038/cdd.2014.169
17. Chen LY, Shieh JJ, Lin B, Pan CJ, Gao JL, Murphy PM, Roe TF, Moses S, Ward JM, Lee EJ, Westphal H, Mansfield BC, Chou JY (2003) Impaired glucose homeostasis, neutrophil trafficking and function in mice lacking the glucose-6-phosphate transporter. Hum Mol Genet 12:2547–2558. https://doi.org/10.1093/hmg/ddg263
18. Kim SY, Jun HS, Mead PA, Mansfield BC, Chou JY (2008) Neutrophil stress and apoptosis underlie myeloid dysfunction in glycogen storage disease type Ib. Blood 111:5704–5711. https://doi.org/10.1182/blood-2007-12-129114
19. Kwon JH, Lee YM, Cho JH, Kim GY, Anduaga J, Starost MF, Mansfield BC, Chou JY (2017) Liver-directed gene therapy for murine glycogen storage disease type Ib. Hum Mol Genet 26:4395–4405. https://doi.org/10.1093/hmg/ddx325
20. Sim SW, Park TS, Kim SJ, Park BC, Weinstein DA, Lee YM, Jun HS (2018) Aberrant proliferation and differentiation of glycogen storage disease type Ib mesenchymal stem cells. FEBS Lett 592:162–171. https://doi.org/10.1002/1873-3468.12939
21. Messina-Graham S, Broxmeyer H (2016) SDF-1/CXCL12 modulates mitochondrial respiration of immature blood cells in

a bi-phasic manner. Blood Cells Mol Dis 58:13–18. https://doi.org/10.1016/j.bcmd.2016.01.008
22. Yiu WH, Pan CJ, Mead PA, Starost MF, Mansfield BC, Chou JY (2009) Normoglycemia alone is insufficient to prevent long-term complications of hepatocellular adenoma in glycogen storage disease type Ib mice. J Hepatol 51:909–917. https://doi.org/10.1016/j.jhep.2008.11.026
23. McDermott DH, De Ravin SS, Jun HS, Liu Q, Priel DA, Noel P, Takemoto CM, Ojode T, Paul SM, Dunsmore KP, Hilligoss D, Marquesen M, Ulrick J, Kuhns DB, Chou JY, Malech HL, Murphy PM (2010) Severe congenital neutropenia resulting from G6PC3 deficiency with increased neutrophil CXCR4 expression and myelokathexis. Blood 116:2793–2802. https://doi.org/10.1182/blood-2010-01-265942
24. Tasseff R, Jensen HA, Congleton J, Dai D, Rogers KV, Sagar A, Bunaciu RP, Yen A, Varner JD (2017) An effective model of the retinoic acid induced HL-60 differentiation program. Sci Rep 7:14327. https://doi.org/10.1038/s41598-017-14523-5
25. Kumar S, Dikshit M (2019) Metabolic insight of neutrophils in health and disease. Front Immunol 10:2099. https://doi.org/10.3389/fimmu.2019.02099
26. Grygiel-Gorniak B (2014) Peroxisome proliferator-activated receptors and their ligands: nutritional and clinical implications—a review. Nutr J 13:17. https://doi.org/10.1186/1475-2891-13-17
27. Christofides A, Konstantinidou E, Jani C, Boussiotis VA (2021) The role of peroxisome proliferator-activated receptors (PPAR) in immune responses. Metabolism 114:154338. https://doi.org/10.1016/j.metabol.2020.154338
28. Schmitz G, Langmann T, Heimerl S (2001) Role of ABCG1 and other ABCG family members in lipid metabolism. J Lipid Res 42:1513–1520
29. Hunt MC, Alexson SE (2002) The role Acyl-CoA thioesterases play in mediating intracellular lipid metabolism. Prog Lipid Res 41:99–130. https://doi.org/10.1016/s0163-7827(01)00017-0
30. Choi SS, Park J, Choi JH (2014) Revisiting PPARgamma as a target for the treatment of metabolic disorders. BMB Rep 47:599–608. https://doi.org/10.5483/bmbrep.2014.47.11.174
31. Dispirito JR, Fang B, Wang F, Lazar MA (2013) Pruning of the adipocyte peroxisome proliferator-activated receptor gamma cistrome by hematopoietic master regulator PU.1. Mol Cell Biol 33:3354–3364. https://doi.org/10.1128/MCB.00599-13
32. Picard F, Kurtev M, Chung N, Topark-Ngarm A, Senawong T, Machado De Oliveira R, Leid M, McBurney MW, Guarente L (2004) Sirt1 promotes fat mobilization in white adipocytes by repressing PPAR-gamma. Nature 429:771–776. https://doi.org/10.1038/nature02583
33. Adams M, Reginato MJ, Shao D, Lazar MA, Chatterjee VK (1997) Transcriptional activation by peroxisome proliferator-activated receptor gamma is inhibited by phosphorylation at a consensus mitogen-activated protein kinase site. J Biol Chem 272:5128–5132. https://doi.org/10.1074/jbc.272.8.5128
34. Camp HS, Tafuri SR (1997) Regulation of peroxisome proliferator-activated receptor gamma activity by mitogen-activated protein kinase. J Biol Chem 272:10811–10816. https://doi.org/10.1074/jbc.272.16.10811
35. Albanesi J, Noguera NI, Banella C, Colangelo T, De Marinis E, Leone S, Palumbo O, Voso MT, Ascenzi P, Nervi C, Bianchi F, di Masi A (2020) Transcriptional and metabolic dissection of ATRA-induced granulocytic differentiation in NB4 acute promyelocytic leukemia cells. Cells. https://doi.org/10.3390/cells9112423
36. Herst PM, Tan AS, Scarlett DJ, Berridge MV (2004) Cell surface oxygen consumption by mitochondrial gene knockout cells. Biochim Biophys Acta 1656:79–87. https://doi.org/10.1016/j.bbabio.2004.01.008
37. Chou JY (2001) The molecular basis of type 1 glycogen storage diseases. Curr Mol Med 1:25–44
38. Eash KJ, Means JM, White DW, Link DC (2009) CXCR4 is a key regulator of neutrophil release from the bone marrow under basal and stress granulopoiesis conditions. Blood 113:4711–4719. https://doi.org/10.1182/blood-2008-09-177287
39. Hong CW (2017) Current understanding in neutrophil differentiation and heterogeneity. Immune Netw 17:298–306. https://doi.org/10.4110/in.2017.17.5.298
40. Dwivedi P, Greis KD (2017) Granulocyte colony-stimulating factor receptor signaling in severe congenital neutropenia, chronic neutrophilic leukemia, and related malignancies. Exp Hematol 46:9–20. https://doi.org/10.1016/j.exphem.2016.10.008
41. Semerad CL, Liu F, Gregory AD, Stumpf K, Link DC (2002) G-CSF is an essential regulator of neutrophil trafficking from the bone marrow to the blood. Immunity 17:413–423. https://doi.org/10.1016/s1074-7613(02)00424-7
42. Guzman M, Lo Verme J, Fu J, Oveisi F, Blazquez C, Piomelli D (2004) Oleoylethanolamide stimulates lipolysis by activating the nuclear receptor peroxisome proliferator-activated receptor alpha (PPAR-alpha). J Biol Chem 279:27849–27854. https://doi.org/10.1074/jbc.M404087200
43. Lefterova MI, Haakonsson AK, Lazar MA, Mandrup S (2014) PPARgamma and the global map of adipogenesis and beyond. Trends Endocrinol Metab 25:293–302. https://doi.org/10.1016/j.tem.2014.04.001
44. Cariou B, Charbonnel B, Staels B (2012) Thiazolidinediones and PPARgamma agonists: time for a reassessment. Trends Endocrinol Metab 23:205–215. https://doi.org/10.1016/j.tem.2012.03.001
45. Croasdell A, Duffney PF, Kim N, Lacy SH, Sime PJ, Phipps RP (2015) PPARgamma and the innate immune system mediate the resolution of inflammation. PPAR Res 2015:549691. https://doi.org/10.1155/2015/549691